行政院國家科學委員會專題研究計畫　成果報告

操作奈米粒子之動力學分析與控制（3/3)

計畫類別：個別型計畫
計畫編號：NSC93-2212-E-009-023-
執行期間：93 年 08 月 01 日至 94 年 07 月 31 日
執行單位：國立交通大學機械工程研究所

計畫主持人：呂宗熙

報告類型：精簡報告

處理方式：本計畫可公開查詢

中　華　民　國 94 年 9 月 30 日

行政院國家科學委員會補助專題研究計畫 ■ 成 果 報 告
□期中進度報告

操作奈米粒子之動力學分析與控制（III）

計畫類別：■個別型計畫　□ 整合型計畫
計畫編號：NSC93－2212－E－009－023
執行期間：　93　年　8　月　1　日至　94　年　7　月　31　日

計畫主持人：　　呂　宗　熙
共同主持人：
計畫參與人員：

成果報告類型(依經費核定清單規定繳交)：■精簡報告　□完整報告

本成果報告包括以下應繳交之附件：
□赴國外出差或研習心得報告一份
□赴大陸地區出差或研習心得報告一份
□出席國際學術會議心得報告及發表之論文各一份
□國際合作研究計畫國外研究報告書一份

處理方式：除產學合作研究計畫、提升產業技術及人才培育研究計畫、列管計畫及下列情形者外，得立即公開查詢
□涉及專利或其他智慧財產權，□一年□二年後可公開查詢

執行單位：　國立交通大學

操作奈米粒子之動力學分析與控制(III)

(國科會計劃編號 NSC93-2212-E-009-023, 執行期限 2004.08.01 ~ 2005.07.31)

呂 宗 熙

新竹市 國立交通大學 機械工程研究所

摘 要

為了機電元件的微小化與生化方面的應用，奈米科技技術運用的重要性也隨著與日俱增。但也由於目前的奈米技術還尚未發展成熟，因此利用奈米操控術來組成奈米級之機電元件與生化 DNA 重組是很重要的研究主題。本研究採用針對模型之不確定性及外界干擾有強健性的順滑模態控制去控制平台，利用閉迴路 X-Y 精密平台的應變計回饋訊號使探針能準確的推動於傾斜面上的奈米粒子。為了補償可能發生的探針與奈米粒子失去接觸，本研究擷取原子力顯微鏡中探針懸臂樑撓曲時，雷射光呈現於四象儀光偵測器的回授電壓訊號，然後使用模糊控制器對此訊號作 X-Y 平台的定位控制，建立一個穩定和高精度的粒子推動系統。

關鍵字： **奈米粒子、 X-Y 精密平台、 奈米操控。**

ABSTRACT

To develop nanotechnology, nanoparticle manipulation plays an important role in the assembly of nanoelements. This study aims to manipulate nanoparticles using an atomic force microscope and an XY positioning stage. Strain gauges serve as sensors to measure the travel distance of piezo-drivers in an X-Y stage in an atomic force microscopy system. Nanoparticles are pushed based on sliding mode control whose robust properties can deal with model uncertainty and disturbance. In addition, a fuzzy controller is responsible for compensating "tip-particle contact loss", so as to establish an accurate and stable manipulation system. Experimental results demonstrate pushing nanoparticles on inclined substrates, different limited scanning ranges with different slope angles, and removing and remaining nanoparticles on inclined substrates.

Keywords: nanoparticle, X-Y stage, nanomanipulation

1. INTRODUCTION

Nano-manipulation using atomic force microscopy (AFM) has attracted much attention among researchers. Sitti and Hashimoto [1] presented that the latex particles with 242- and 484-nm radii can be positioned on a Si substrate successfully at around 30-nm accuracy. In another work of Sitti [2], 500-nm radius gold-coated latex particles are pushed on a silicon substrate. Frictional parameters and behavior are estimated using the proposed models and experimental pushing force data.

In this study, manipulation of nanoparticles in 3-D is carried out based on previous investigation results in 1-D and 2-D. An X-Y stage is moved by utilizing a sliding-mode control (SMC) controller to position a nanoparticle. But during pushing, a nanoparticle is unlikely pushed along the predictable direction. That is, the tip-particle contact can be lost due to X-Y stage positioning errors, and the rotation/spinning of the particle. Therefore, a fuzzy controller will compensate these positioning errors according to photodetector feedback signals of AFM.

In order to make 3-D movement of nanoparticles, the height between the substrate and X-Y stage has to be adjusted. Moreover, the difference between pushing up and pushing down will be observed, and which way is easier to push will be discussed. Finally, experimental results demonstrate pushing nanoparticles on an inclined substrate, the limitation of scanning range in different inclinations, and removed and remained nanoparticles on the inclined substrate.

2. MANIPULATION STRATEGY

In this study, golden nanoparticles on a Si substrate are to be pushed using a Si fabricated AFM cantilever tip in ambient conditions. At first, the image of nanoparticle is obtained using AFM semicontact-mode imaging, and then using contact-mode may move the nanoparticles. Assuming the particle is pushed along the y-axis or x-axis, this study deals with two-dimensional (2-D) pushing strategy.

2.1 Pushing Scheme in 1-D

Motion steps that realize AFM-based pushing in y-axis or x-axis are shown in Fig. 1 with an angle θ, where F denotes the farther final position of the particle in pushing down.

1.<1→2>: The tip is moved along the z direction until detecting the contact with the substrate by measuring the cantilever deflection (absolute tip-substrate distance is not known initially), and retracted back to a predetermined parking height h_{set}.
2.<2→3>: The substrate is moved along the desire direction until detecting the contact between the tip and the particle by cantilever deflection detection, and then stopped.
3.<3→5>: The particle can be pushed for a maximum

distance Δd_{max} by moving the substrate due to the inclination of the substrate.

In Step 2, the tip and particle may lose contact due to positioning errors, and particle rotation/spinning along the z-axis during pushing. Once it occurs, y-axis or x-axis motion should stop, and the substrate must return to the position where contact loss begins by two axes controllers. In Step 3, the pushing scheme is repeated until there is no contact loss.

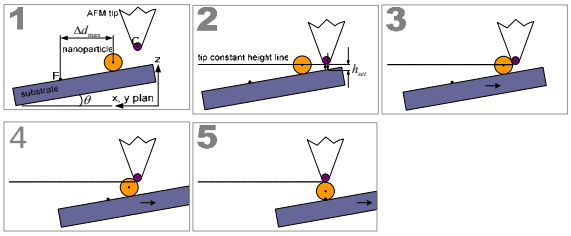

Fig. 1 AFM-based 2-D particle pushing strategy.

The tip is not raised or lowered during pushing in AFM contact mode. That is, when substrate tilts, the tip is kept horizontal during pushing. Accordingly, the tip and particle in pushing down would lose contact inevitably. Therefore, there is the maximum distance in pushing the gold nanoparticle down the inclined substrate, as shown in Fig 2. The maximum distance is written as

$$\Delta d_{\max} + \Delta d_{ta} \cong \frac{2R_a - h_{set}}{\tan\theta} \qquad (1)$$

where Δd_{max} is the original distance between AFM tip and particle, Δd_{ta} is the maximum distance of the particle pushing, R_a is the particle radius, h_{set} is predetermined parking height, and θ is the inclination of the substrate.

According to this pushing strategy, pushing up can succeed easier than pushing down obviously. Certainly, Eq. (1) ignores the nanoparticle sprung by AFM probe tip and rolling itself. Moreover, assuming the particle is purely sliding and the substrate is smooth enough.

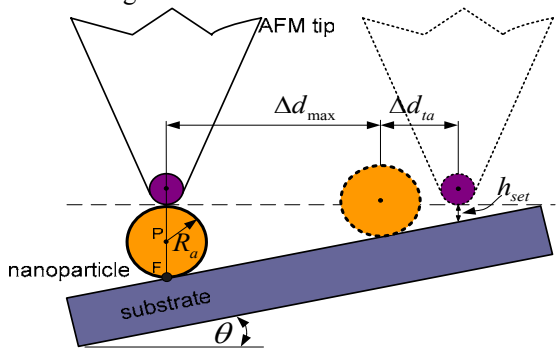

Fig. 2 Maximal distance in pushing the particle down.

In order to create the inclination angle at 1°, 2°, and 3°, we have to pad the substrate high , for example, tan1° ≒ 0.0175, tan2° ≒ 0.0349, and tan3° ≒ 0.0524. As a consequence, when the width of the bottom is 10000 nm, the heights become 175 nm, 349 nm, and 524 nm, respectively. If parameter values are selected as follows: θ = 0.1°~3°, R_a=50nm, and h_{set}=0~100 nm. Substituting these parameters into Eq. (1) is depicted in Fig. 3. The inclination variation of the substrate will be illustrated in chapter 5.

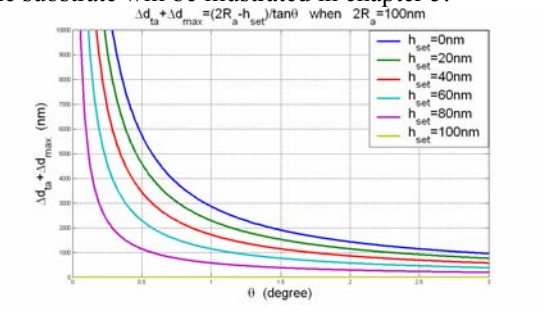

Fig. 3 Relation among the maximal distance in pushing the nanoparticle down, the substrate inclination angle, and the predetermined parking height.

2.2 Pushing Scheme in 2-D

After AFM imaging, the tip is located above and to the conter of the image coordinates with a preset value of the center of the image coordinates with a preset value of $z_{park} = z_c + h_{set}$ where z_c is the final tip-substrate contact z position. The resulting AFM image frame coordinates and components in the 2-D graphics user interface can be seen in Fig. 4. (x, y) denotes the AFM image coordinate frame with nanometer units, and (X, Y) stands for the stage x-y nanometer position coordinates. The relation between both coordinates can be given as

$$(X, Y) = (x+Xo, y+Yo)$$

where (X_o, Y_o) are the initial positions during the AFM imaging. The points O, P, and T in Fig. 2.4 represent the AFM tip center, manually selected particle center, and user-defined target position, respectively. The aim of the automatic control scheme is "to push the particle at P to the point T precisely." Assuming the stage x-y positioning is precise due to closed-loop control, and the substrate is moved instead of the AFM tip where the tip behaves as a stopper during pushing, the proposed pushing scheme for enabling this control is as follows.

1. Initially, (x_o, y_o)=(N_x/2, N_y/2) where N_x and N_y are the AFM image x and y nanometer sizes, and (x_p, y_p) and (x_T, y_T) points are known. Thus, the distance ΔL, the pushing direction θ, and the initial approach point A coordinates are computed as

$$(\Delta x, \Delta y) = (x_T - x_p, y_T - y_P)$$
$$\Delta L = \sqrt{\Delta x^2 + \Delta y^2}$$
$$\theta = \arctan(|\Delta y|/|\Delta x|)$$
$$(s_x, s_y) = (|\Delta x|/\Delta x, |\Delta y|/\Delta y)$$
$$(x_A, y_A) = (x_O + s_x R\sin\theta, y_O + s_y R\cos\theta)$$

   where $R = 3R_a + R_t$

2. Initial positioning before pushing: move stage from P to A by setting (X, Y) = (X_o+x_A-x_p, Y_o+y_A-y_p).

3. Contact point B detection: move from A through O.
4. Contact pushing through the point C, i.e., $(x_C, y_C) = (x_B - s_x \Delta L\cos\theta, y_B - s_y \Delta L\sin\theta)$.
5. Returning to the initial positions: move stage to (X_o, Y_o) and automatically park to the z_{park} height.

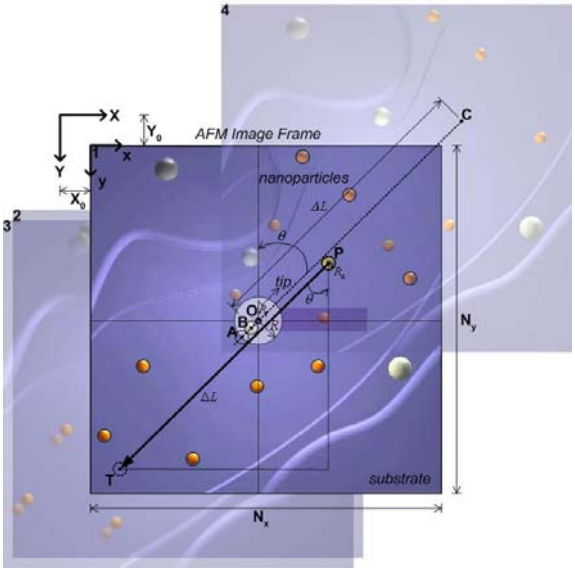

Fig. 4 Coordinate frames in 2-D AFM image display.

2.3.1 AFM Dynamic Plant

To illustrate AFM dynamic plant, consider the system described by

$$\begin{cases} m_{x-eff}\ddot{y}_x + b_x\dot{y}_x + k_x y_x = F_x - f_{as} \\ m_{y-eff}\ddot{y}_y + b_y\dot{y}_y + k_y y_y = F_y - f_{as} \end{cases} \quad (2)$$

where $m_{x\text{-}eff}$ and $m_{y\text{-}eff}$ are effective masses, b_x and b_y are viscous coefficients , and y_x and y_y are positions of x-axis and y-axis in XY stage, respectively. $k_x = k_y = 15\times10^6$ N/m are stiffness coefficients of two PZT translators of the XY scanning stage. F_x and F_y are the stage driving force in x-direction and y-direction, and f_{as} is a friction force between the particle and substrate. In Eq. (2),

$$b = 2\xi\sqrt{km_{eff}} \quad (3)$$

$$m_{eff} = \frac{k}{\omega_n^2} \quad (4)$$

where ξ and ω_n are damping ratio and natural frequency, respectively. To measure ξ and ω_n, the equations of

$$\omega_n = \frac{2\pi f_r}{\sqrt{1-2\xi^2}} \quad (5)$$

$$\sigma = \omega_n\xi \quad (6)$$

will be utilized, where f_r and σ are resonance frequency and damping factor, respectively. Substituting values of f_r, σ, ξ, m_{eff}, and b in Tables 1 and 2 to Eqs. (3), (4), (5), and (6), parameters of $m_{x\text{-}eff}$= 0.0905 Kg, $m_{y\text{-}eff}$=0.1262 Kg, b_x= 821.0602 Kg/s and b_y=965.9074 Kg/s are obtained. According to Sitti and Hashimoto [1], f_{as}=1.611×10^{-8} N is used for Eq. (2). As a result, the equation of motion for the AFM system can be obtained as

$$\begin{cases} 0.0905\ddot{y}_x + 821.0602\dot{y}_x + 15\times10^6 y_x = F_x - 1.611\times10^{-8} \\ 0.1262\ddot{y}_y + 965.9074\dot{y}_y + 15\times10^6 y_y = F_y - 1.611\times10^{-8} \end{cases} \quad (7)$$

Table 1 Values of f_r, σ, ξ, m_{eff}, and b for X-axis.

Parameters	f_r (Hz)	σ	ξ	m_{eff} (Kg)	b (Kg/s)
Values	1777	4583.3	0.35375	0.090464	821.0600

Table 2 Values of f_r, σ, ξ, m_{eff}, and b for Y-axis.

Parameters	f_r (Hz)	σ	ξ	m_{eff} (Kg)	b (Kg/s)
Values	1493.25	3872.8	0.35222	0.126163	965.9077

2.3.2 XY Stage

According to Section 2.2, the piezoelectric translator of the X-Y stage is the core of actuating element. The X-Y stage system consists of piezoelectric and mechanical parts. In this study, nanoparticle manipulation is performed at very slow velocity and PZT translator is a high-resolution linear actuator for static and dynamic applications. Therefore, the hysteresis and creep of piezoelectric translators will be neglected. Because all electric energies are transferred into mechanical energy, generated mechanical force can be written as

$$F = K_p dL(t) \quad (8)$$

where $dL(t)$ can be expressed by

$$dL(t) = S_p V(t) \quad (9)$$

where K_p is the spring constant of piezoelectric translator, $dL(t)$ is the elongation of PZT translator subject to voltage, S_p is a piezoelectric strain constant and $V(t)$ is input voltage, respectively. Both piezoelectric translators are in full extension, such that the XY stage is located at the maximum X and Y positions in initial state. The model combines the x and y components, the mechanical force can be modified as

$$\begin{cases} F_x = k_x dL_x(t) \\ F_y = k_y dL_y(t) \end{cases} \quad (10)$$

where F_x and F_y are x and y components of generation force of the XY stage, respectively, k_x and k_y are X-axis and Y-axis spring constants of the XY stage, respectively, $dL_x(t)$ and $dL_y(t)$ can also be expressed as, respectively, from Eq. (8),

$$\begin{cases} dL_x(t) = S_{p-x}V_x(t) \\ dL_y(t) = S_{p-y}V_y(t) \end{cases} \quad (11)$$

where $S_{p\text{-}x}$ and $S_{p\text{-}y}$ are x-axis and y-axis of piezoelectric-strain constants of the XY scanning stage, respectively, and $V_x(t)$ and $V_y(t)$ are X-axis and Y-axis of an input voltage. Substituting Eq (11) into Eq. (10) leads to XY stage force:

$$\begin{cases} F_x = k_x S_{p-x}V_x(t) \\ F_y = k_y S_{p-y}V_y(t) \end{cases} \quad (12)$$

where $S_{p\text{-}x}$ and $S_{p\text{-}y}$ can be obtained by measuring position and piezo voltage. Measurement results and linear fit of the results are shown as Figs. 5 and 6,

from which linear-fit equations read

$$\begin{cases} Position_x = 1100\, Voltage_x + 2200 \\ Position_y = 1200\, Voltage_y + 20000 \end{cases} \quad (13)$$

where displacements of $Position_x$ and $Position_y$ can be described as $dL_x(t)$ and $dL_y(t)$, respectively. Therefore, $S_{p\text{-}x}$ = 1100 nm/v, $S_{p\text{-}y}$ = 1200 nm/v, and $k_x = k_y = 15\times10^6$ N/m- are obtained from Eq. (12), Eq. (13), Fig. 5. Substituting $S_{p\text{-}x}$, $S_{p\text{-}y}$, k_x and k_y into Eq. (12) yields modeling of the XY stage system as

$$\begin{cases} F_x = \tau_x = 16.5\, V_x + 33 \\ F_y = \tau_y = 18\, V_y + 300 \end{cases} \quad (14)$$

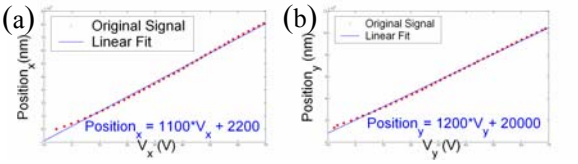

Fig. 5 Linear fit of voltage vs. position (a) X-axis (b) Y-axis.

2.4 System Plant Model

According to Fig. 6, the system plant consists of an AFM dynamic plant and an XY stage system. From Sections 2.3.1 and 2.3.2, substituting Eq. (14) into (7) and altering the unit of y from meter to nanometer, the system plant model yields

$$\begin{cases} 0.0905\times10^{-9}\, \ddot{y}_x + 821.0602\times10^{-9}\, \dot{y}_x + 15\times10^{-3}\, y_x \\ = 16.5\, V_x + 33 - 1.611\times10^{-8} \\ 0.1262\times10^{-9}\, \ddot{y}_y + 965.9074\times10^{-9}\, \dot{y}_y + 15\times10^{-3}\, y \\ = 18\, V_y + 300 - 1.611\times10^{-8} \end{cases} \quad (15)$$

Because $33 >> 1.611\times10^{-8}$ and $300 >> 1.611\times10^{-8}$ in (15), terms 1.611×10^{-8} will be ignored and system plant model can be given as

$$\begin{cases} 0.0905\times10^{-9}\, \ddot{y}_x + 821.0602\times10^{-9}\, \dot{y}_x + 15\times10^{-3}\, y_x - 33 \\ = 16.5\, V_x \\ 0.1262\times10^{-9}\, \ddot{y}_y + 965.9074\times10^{-9}\, \dot{y}_y + 15\times10^{-3}\, y - 300 \\ = 18\, V_y \end{cases} \quad (16)$$

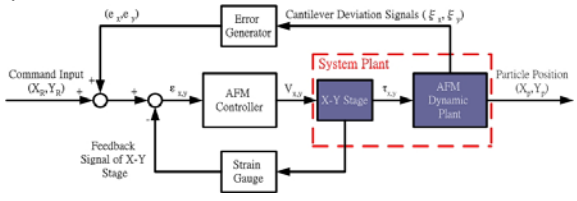

Fig. 6 Original control system diagram.

2.5 Discrete Time System Plant

In this study, the system plant model will be transformed from continuous-time domain into discrete-time domain.

At first, Eq. (16) is modified as

$$\begin{cases} 6.0333\times10^{-9}\, \ddot{y}_x + 5.4737\times10^{-5}\, \dot{y}_x + y_x - 2.2\times10^3 \\ = 1.1\times10^3 V_x \\ 8.4133\times10^{-9}\, \ddot{y}_y + 6.4394\times10^{-5}\, \dot{y}_y + y_y - 2\times10^3 \\ = 1.2\times10^3 V_y \end{cases} \quad (17)$$

For simplicity, denote y_x' and y_y' for y_x-2.2×10^3 and y_y-2×10^3, respectively. Therefore,

$$\begin{cases} y_x' = y_x - 2.2\times10^3 \\ \dot{y}_x' = \dot{y}_x \\ \ddot{y}_x' = \ddot{y}_x \end{cases} \text{ and } \begin{cases} y_y' = y_y - 2\times10^3 \\ \dot{y}_y' = \dot{y}_y \\ \ddot{y}_y' = \ddot{y}_y \end{cases} \quad (18)$$

Substituting Eq. (18) into Eq. (17) yields

$$\begin{cases} 6.0333\times10^{-9}\, \ddot{y}_x' + 5.4737\times10^{-5}\, \dot{y}_x' + y_x' \\ = 1.1\times10^3 V_x \\ 8.4133\times10^{-9}\, \ddot{y}_y' + 6.4394\times10^{-5}\, \dot{y}_y' + y_y' \\ = 1.2\times10^3 V_y \end{cases} \quad (19)$$

Second, the Laplace transform of Eq. (19) is written as

$$\begin{cases} 6.0333\times10^{-9}\, s^2 Y_x'(s) + 5.4737\times10^{-5}\, s Y_x'(s) + Y_x'(s) \\ = 1.1\times10^3 V_x(s) \\ 8.4133\times10^{-9}\, s^2 Y_y'(s) + 6.4394\times10^{-5}\, s Y_y'(s) + Y_y'(s) \\ = 1.2\times10^3 V_y(s) \end{cases} \quad (20)$$

Hence, the transfer function of system plant is

$$\begin{cases} P_x(s) = \dfrac{Y_x'(s)}{V_x(s)} = \dfrac{1.1\times10^3}{6.0333\times10^{-9} s^2 + 5.4737\times10^{-5} s + 1} \\ P_y(s) = \dfrac{Y_y'(s)}{V_y(s)} = \dfrac{1.2\times10^3}{8.4133\times10^{-9} s^2 + 6.4394\times10^{-5} s + 1} \end{cases} \quad (21)$$

The system plant of Eq. (21) can be converted to state-space form as

$$\begin{cases} \begin{cases} \dot{X}_x = A_x X_x + B_x u_x \\ y_x' = C_x X_x + D_x u_x \end{cases} \\ \begin{cases} \dot{X}_y = A_y X_y + B_y u_y \\ y_y' = C_y X_y + D_y u_y \end{cases} \end{cases} \quad (22)$$

where $A_x = \begin{bmatrix} -9.0725\times10^3 & -1.6575\times10^8 \\ 1 & 0 \end{bmatrix}$, $B_x = \begin{bmatrix} 1 \\ 0 \end{bmatrix}$, $C_x = \begin{bmatrix} 0 & 1.8232\times10^{11} \end{bmatrix}$ and $D_x = 0$, and $A_y = \begin{bmatrix} -7.6538\times10^3 & -1.1886\times10^8 \\ 1 & 0 \end{bmatrix}$, $B_y = \begin{bmatrix} 1 \\ 0 \end{bmatrix}$, $C_y = \begin{bmatrix} 0 & 1.4263\times10^{11} \end{bmatrix}$ and $D_y = 0$. $y_x' \in R$ and $y_y' \in R$ denote plant output related to the x and y positions of the XY stage, respectively, $u_x \in R$ and $u_y \in R$ are the control input voltage of x and y-axes respectively.

Third, the system plant of Eq. (22) will be converted to discrete-time domain by Z-transform method at 5K sampling rate. The Z-transform of the system plant is obtained as

$$\begin{cases} \begin{cases} X_x(k+1) = A_{zx} X_x(k) + B_{zx} u_x(k) \\ y_x'(k) = C_{zx} X_x(k) + D_{zx} u_x(k) \end{cases} \\ \begin{cases} X_y(k+1) = A_{zy} X_y(k) + B_{zy} u_y(k) \\ y_y'(k) = C_{zy} X_y(k) + D_{zy} u_y(k) \end{cases} \end{cases} \quad (23)$$

where $A_{zx} = \begin{bmatrix} -4.0183\times10^{-1} & -3.7106\times10^{3} \\ 2.2387\times10^{-5} & -1.9872\times10^{-1} \end{bmatrix}$,

$B_{zx} = \begin{bmatrix} 2.2387\times10^{-5} \\ 7.2322\times10^{-9} \end{bmatrix}$, $C_{zx} = \begin{bmatrix} 0 & 1.8232\times10^{11} \end{bmatrix}$ and

$D_{zx} = 0$, and $A_{zy} = \begin{bmatrix} -3.6644\times10^{-1} & -4.8264\times10^{3} \\ 4.0606\times10^{-5} & -5.5645\times10^{-2} \end{bmatrix}$,

$B_{zy} = \begin{bmatrix} 4.0606\times10^{-5} \\ 8.8815\times10^{-9} \end{bmatrix}$, $C_{zy} = \begin{bmatrix} 0 & 1.4263\times10^{11} \end{bmatrix}$ and

$D_{zy} = 0$. According to Eq. (23), both ranks of the controllability and observability matrices are 2. Hence, two axes of the system are both controllable and observable.

3. PUSHING CONTROL METHODS

An XY stage is actuated to achieve nanoparticle manipulation by sliding mode control (SMC) [3]. SMC has been known as an effective approach to position and velocity control due to its insensitivity to parameter variations and disturbance rejection capability. Hence, this research designs a sliding mode controller as shown in Fig. 7 for nanoparticle manipulation. In practice, a discrete linear time-invariant system sometimes has system disturbances and measurement noise. Hence, here linear quadratic estimator (LQE) will be applied to estimate optimal states in having system disturbances and measurement noise.

In Fig. 8, in addition to tip-particle contact loss or other operating errors during pushing of nanoparticles also influences plant performance. Therefore, these error sources will be analyzed and compensated by fuzzy controller.

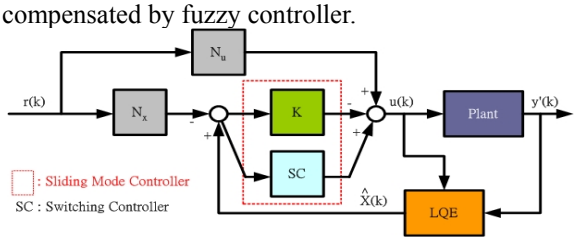

Fig. 7 SMC block diagram with LQE.

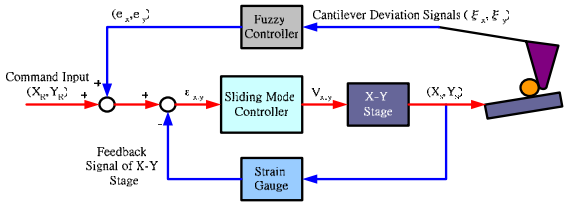

Fig. 8 Control system for pushing particles.

4. SIMULATION RESULTS

In order to manipulate nanoparticles, SMC and FLC will be integrated to control the stage in this study. Therefore, simulation results of the nanoparticle manipulation with SMC and FLC controllers will be presented in this section. The flow chart of the nanoparticle manipulation with the SMC based on LQE and FLC controllers is shown in Fig. 9. The reference chart of tip, particle, and pushing direction is depicted in Fig. 10.

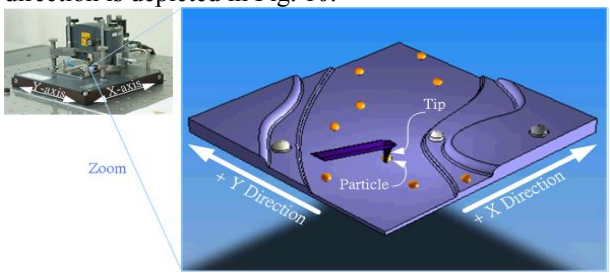

Fig. 9 Coordinate axes definition.

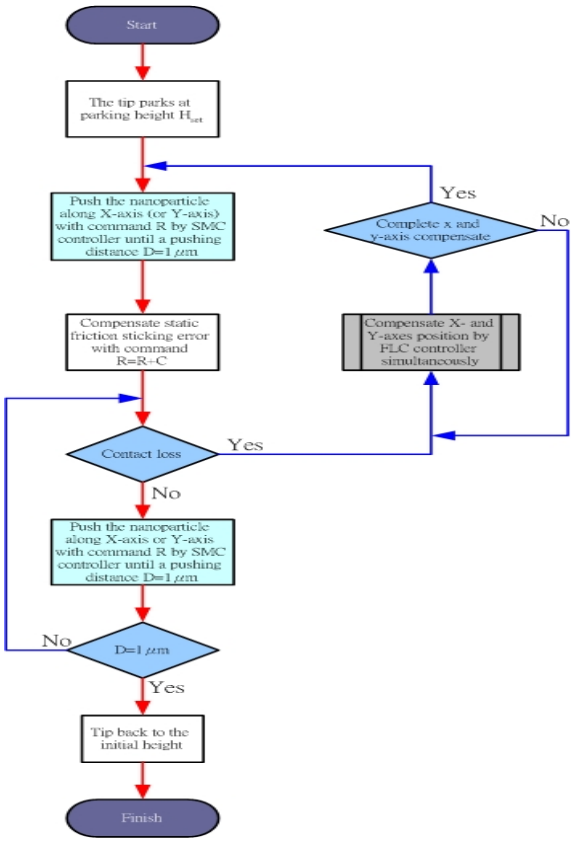

Fig. 10 Flow chart of nanoparticle manipulation.

Simulation conditions are assumed as follows:

1. Command input starts to send at 0.01 sec and tip-particle contact loss occurs at 0.0102, 0.0112, 0.0124, and 0.0138 seconds.
2. In addition to tip-particle contact loss, static friction sticking will also occur when pushing nanoparticle at the beginning motion, which consists of initial. In this study, assuming static friction sticking needs a compensated value of 30 nm for pushing along pure X– or Y–direction. And for simply comparison, compensated value is around 21 nm for XY direction individually.

3. In this study, assuming along XY–direction push a distance 100 nm to X and Y simultaneously.

Simulation results by using software MATLAB and SIMULINK are shown in Fig. 11, where solid line is reference command input whereas the dashed line is output response.

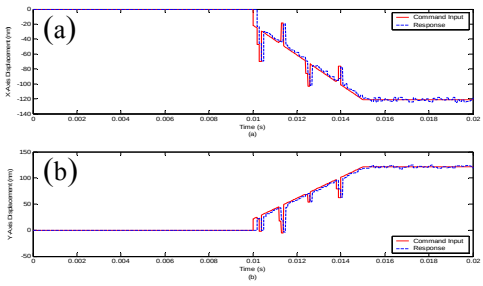

Fig. 11 Simulation results for pushing along +X–Y–direction (a) in X-Axis (b) in Y-Axis.

5. EXPERIMENTAL RESULT

5.1 Lateral Size of Nanoparticle

The measured height of the particles is around 100 nm and the width around 500 nm. However, it should be kept in mind that AFM images are convolutions of the samples and tip geometries [4], which gives a correct height but an overestimated width of the imaged features. The ability to manipulate the particles on the surface supplies a simple way of getting around this problem:

The total widening $2\times w$ of individual particle in Fig. 12 (f) is the same as two particles of similar shape and height lying close together in Fig. 12 (c). Thus by measuring the width of two particles separately and before they have been pushed away, we are able to estimate their lateral size. Each particle in Fig. 12 (e) appears as 500 nm wide, whereas the joined particles in Fig. 12 (b) are only 600 nm together. We have lost $2\times w$ of widening in between them in Fig. 12 (c). Lateral size of one of the particles in Fig. 12 (e) is the total width in Fig. 12 (b) (600 nm) subtracted with the width of the particle is 100 nm.

AFM images result from not only convolutions of samples and tip geometries, but also the XY-stage step distance. About XY stage step distance is shown in Table 3. According to Table 3, XY stage step distance is around 33.3 nm under $10\mu m\times 10\mu m$ scanning scale.

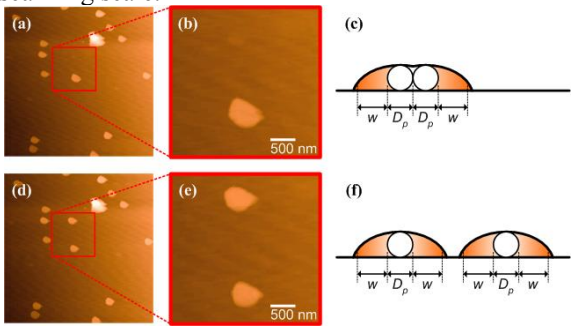

Fig. 12 Illustration of lateral sizes.

Table 3 Step distance of XY stage under different scale scanning.

Step	Scale
0.25 $\mathring{A}$	$0.01\times 0.01\mu m$
1.05 $\mathring{A}$	$0.03\times 0.03\mu m$
5.0 $\mathring{A}$	$0.15\times 0.14\mu m$
10.0 $\mathring{A}$	$0.30\times 0.28\mu m$
50.0 $\mathring{A}$	$1.5\times 1.4\mu m$
100.0 $\mathring{A}$	$3.0\times 2.8\mu m$
500.0 $\mathring{A}$	$15\times 14\mu m$
1000.0 $\mathring{A}$	$30\times 28\mu m$
3495.25 $\mathring{A}$	$105\times 97\mu m$

5.2 Adhesion Effect

In our attempt to nanoparticle pushing in contact mode, we found that they are very easily picked up by the tip as it moves across nanoparticles. Most often this is an unwanted effect, which makes stable imaging impossible.

Examples on a test are shown in Fig. 13, a series of AFM pictures where the gold nanoparticles were adsorbed by the tip. All images in Fig. 13 were recorded using the tapping mode and manipulated using the contact mode. The white solid and the gray dotted arrows represent the planned pushing directions and the planned movements of the particles, respectively. In Fig. 13 (a) and (b) particle 1 vanished since it is adsorbed by the tip right-front side. For this reason, overlapping image occurs. That is, each raised objects in Fig. 13 (b) seemed to add one raised object at left-down side. Particles 2, 3, and 4 were adsorbed as the same manipulation as particle 1 in Fig. 13 (b), (c), and (d), respectively. Hence, each raised objects in Fig. 13 (e) seemed to add three raised objects left side and one right side due to three times from left to right and one time from right to left planned pushing.

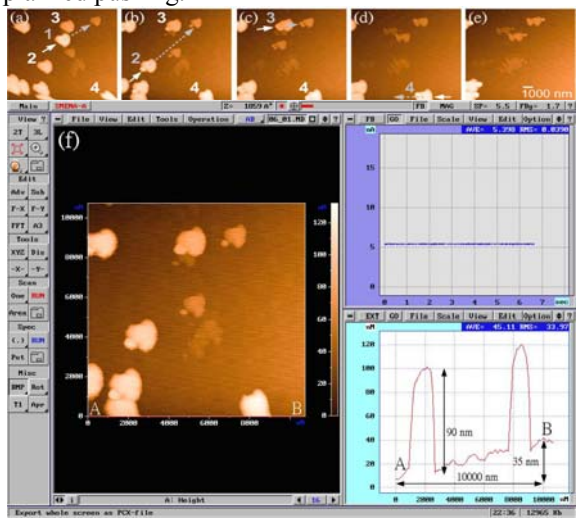

Fig. 13 Effect of adhesion
(a) to (e) series pushing; (f) zoom in (b).

Above phenomenon happens in Sections 5.5 and 5.6.

5.3 Manipulation I

In Fig. 14, the inclination of the substrate is atan(40/10000)≒0.23° in x-direction and the gold nanoparticle is about 100 nm height. Under inclined substrate, a pushing manipulation proceeded following.

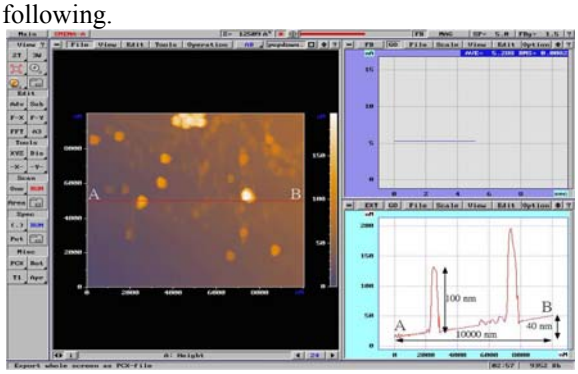

Fig. 14 Inclination of substrate and height of gold nanoparticle.

A gold nanoparticle is pushed up the inclined substrate three times to achieve the target I in Fig. 15, and the particle is pushed down the inclined substrate six times to achieve the target II in Fig. 16. Above manipulation is done by the vector lithography. Distance of a nanoparticle pushed to target I is around 5600 nm in Fig. 15. Another distance of nanoparticle pushed to target II is around 4500 nm in Fig. 16. Average displacements of up and down the inclined substrate are 1867 nm and 720 nm, respectively. According to above manipulation result, pushing up is easier to target than pushing down probably.

In this experiment, the angle of the inclination θ is 0.23°, and the diameter $2R_a$ of nanoparticle is 100 nm. Substituting parameters into Eq. (1) would yield $\Delta d_{ta}+\Delta d_{max}$ about 24911 nm with h_{set} = 80 nm in pushing down under none contact loss condition of tip-particle. Hence, manipulation in Fig. 16 appeared on contact loss of tip-particle.

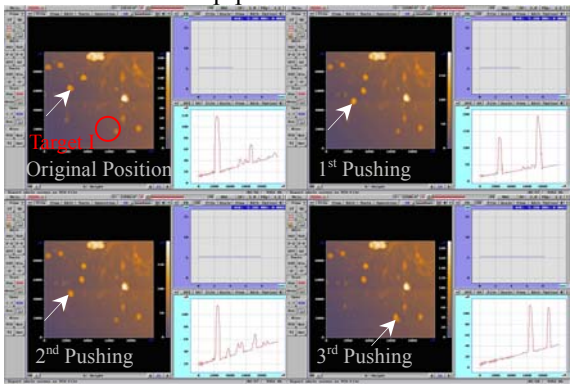

Fig. 15 Three times of pushing up process and corresponding X-direction profile.

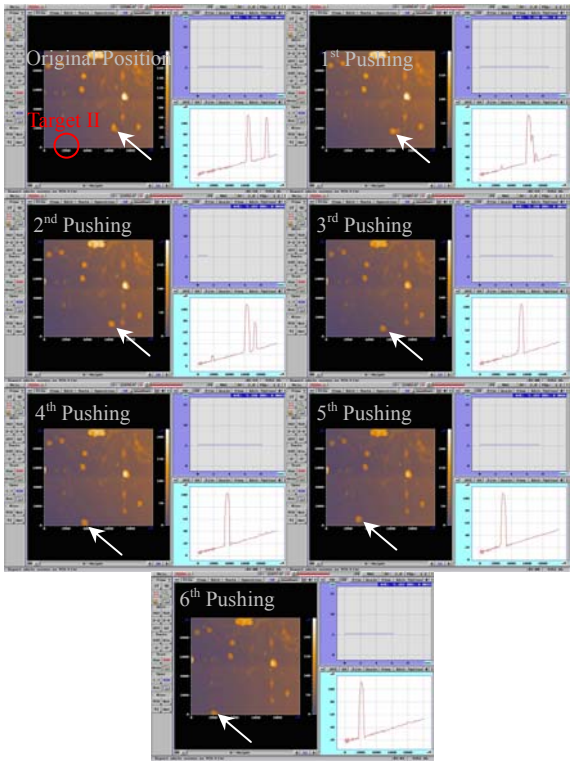

Fig. 16 Six times of pushing down process and corresponding X-direction profile.

5.4 Limitation of Scanning Range

Fig. 17, where padding one, two, and three pieces of paper of thickness 0.6 mm in y-direction makes the inclination angle at the average 0.85°, 1.59°, and 2.12°, respectively.

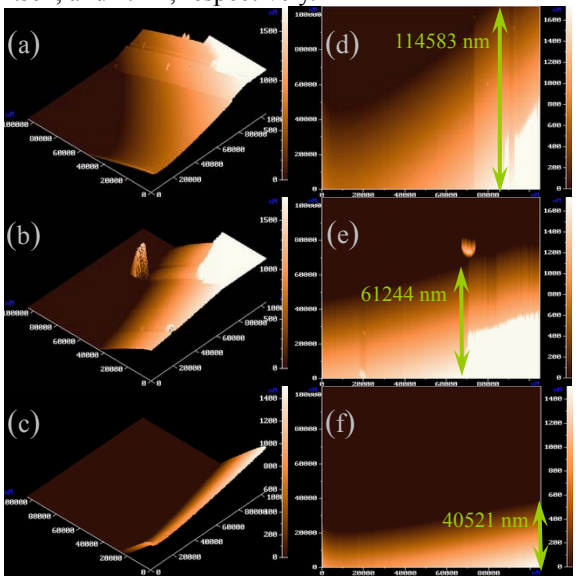

Fig. 17 3-D topography of padding (a) 1 paper at angle 0.85° (b) 2 paper at angle 1.59° (c) 3 paper at angle 2.12° and limited scanning range of (d) 114583nm (e) 61244nm (f) 40521nm.

According to above result, adding paper can raise the inclination angle and limit height range to 1600 nm. That is, higher than height 1600 nm and lower than height 0 nm topography can not be recorded by AFM tapping mode under none adjusted inner setting.

Due to the height limitation, the scanning range at y-coordinate is also limited, respectively. As shown in Fig. 17, the scanning range at y-coordinate is limited to $1700\times(\tan 0.85^{o})^{-1} \fallingdotseq 114583$, $1700\times(\tan 1.59^{o})^{-1} \fallingdotseq 61244$, and $1500\times(\tan 2.12^{o})^{-1} \fallingdotseq 40521$, respectively. According to above experimental results, the relation of inclination angle and limited scanning range is plotted in Fig. 18 where shows the more inclined it is, the less the scanning range is obtained. As a consequence, the scanning range is limited to $\theta \leqq 2.86^{o}$. That is, AFM is neither recording any topography nor doing about pushing particle when $\theta \leqq 2.86^{o}$.

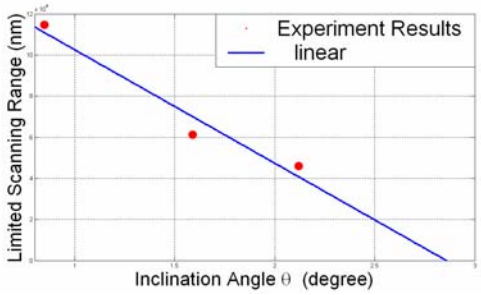

Fig. 18 Relation of inclination angle and limited scanning range.

5.5 Manipulation II

A manipulation example on a Si sample surface is shown in Fig. 19, which displays a series of AFM pictures where gold nanoparticles were removed limited only by the size of the scan range.

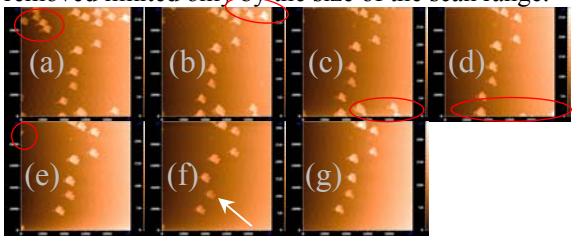

Fig. 19 Removing minor nanoparticles and remaining main ones.

All images in Fig. 19 were recorded using the tapping mode while nanoparticles were pushed in the contact mode. Fig. 19 shows the nanoparticles on the borderland deposited forming the Dipper and also shows that the substrate higher in the right side and lower in the left side. As depicted in Figs. 19 (a) to (e), the red ovals represent the nanoparticles pushed away afterwards. In Fig. 19 (f) the white arrow shows a nanoparticle subject to unexpected pushing and is to be pushed back to the original position. In Fig. 19 (g) the new position of the nanoparticles is indicated. Fig 20 shows the 3-D topography of Fig. 19 (g) and the profile cross-section of the white line.

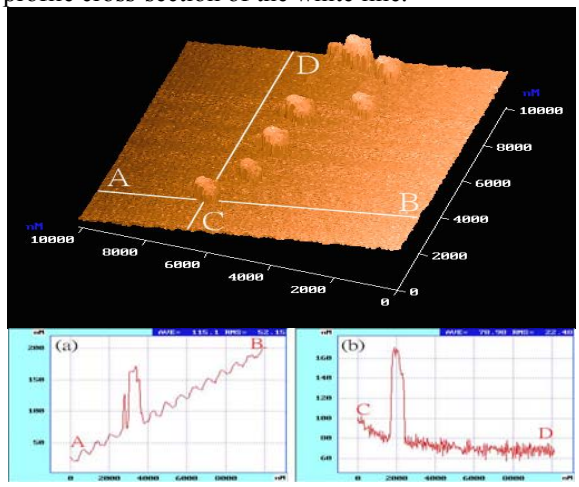

Fig. 20 3-D topography of Fig. 19 (g) and cross-section of (a) AB (b) CD.

5.6 Manipulation III

Another manipulation result on a Si sample surface is shown in Fig. 21 where gold nanoparticles were pushed to form a Chinese word “呂”.Fig. 21 (a) depicts a scheme of positioning nanoparticle targets. A series process of achieving Fig. 21 (b) is shown in Fig. 22. All images in Fig. 22 were recorded using the tapping mode while nanoparticles were pushed in AFM contact mode.

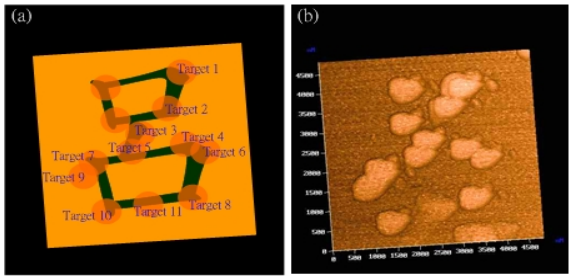

Fig. 21 (a) Pushing scheme (b) Topography in picture 104 of Fig. 22.

Before describing Fig. 22, signs are defined as following:

1. Target numbers and red circles show positioning nanoparticle locations in sequence.
2. Gray arrows show pushing direction.
3. Dotted white circles show adsorbed nanoparticle by a tip or nearby particle.

Fig. 29 will be divided into three parts to describe as following:

Part 1. From picture 1 to 40, pushing particles forms upper “呂” such as “口”. Using seven times position a nanoparticle to target 1 from Picture 1 to 7, four times position a nanopartcle to target 2 from Pictures 8 to 11, and one time position a nanoparticle to target 3 at Picture 12. Pictures 14 and 15 show that three nanoparticles adsorbed by a tip and two nearby nanoparticles.

Overlapping image occurs due to a nanoparticle adsorbed by the tip. That is, each raised objects at Picture 16 seemed to add one raised object at right-down side. From Pictures 17 to 26, repeating process position a nanoparticle to target 2, which used ten times to achieve. A nanoparticle was pushed to target 3 from Pictures 27 to 34 and adsorbed by particle at Picture 35. Another nanoparticle was adsorbed by tip at Picture 38.

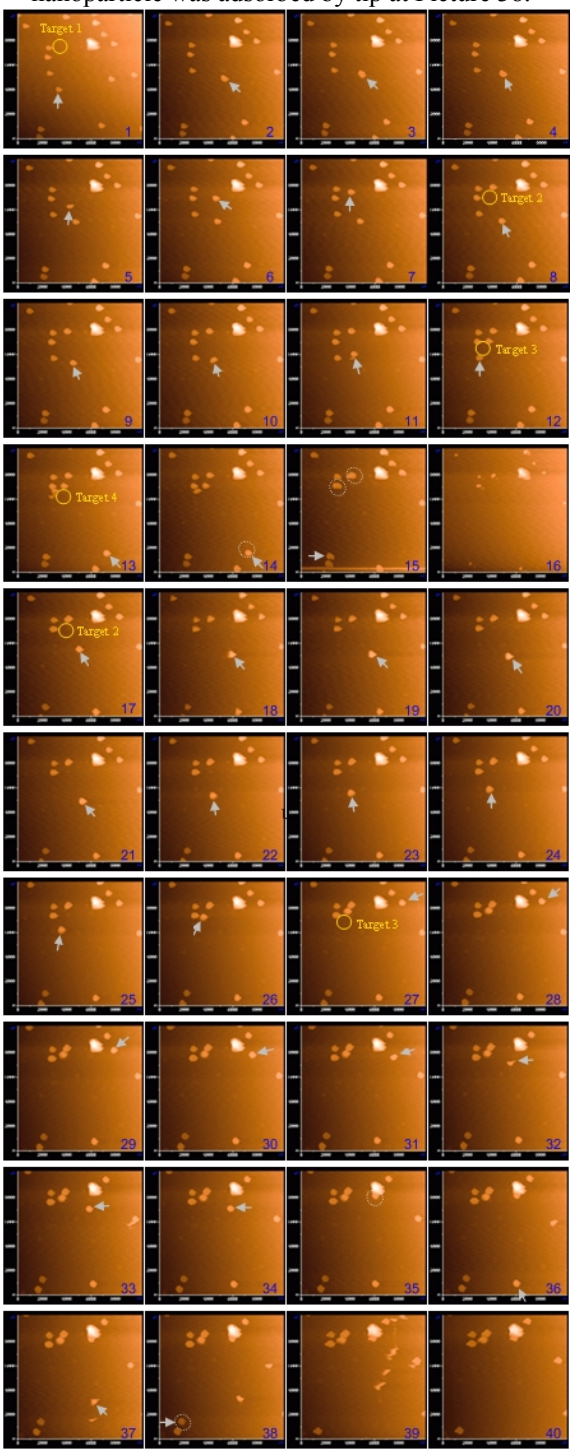

Part 2. From picture 41 to 77, pushing particles forms lower “呂”. Using six times position a nanoparticle to target 3 from Pictures 43 to 48. At Picture 49, a nanoparticle is adsorbed by the tip. Using five times position a nanoparticle to target 4. During pushing nanoparticle to target 5, three nanoparticles was adsorbed by the tip at Pictures 55, 56, and 58. Using two times position a nanoparticle to target 5 from Pictures 61to 62. Also using two times position a nanoparticle to target 6 from Picture 63 to 64. Using four times position a nanoparticle to target 7 from Pictures 66 to 69. Processes of positioning nanoparticles to targets 8, 9, and 10 are not stored up comletely due to the computer crash.

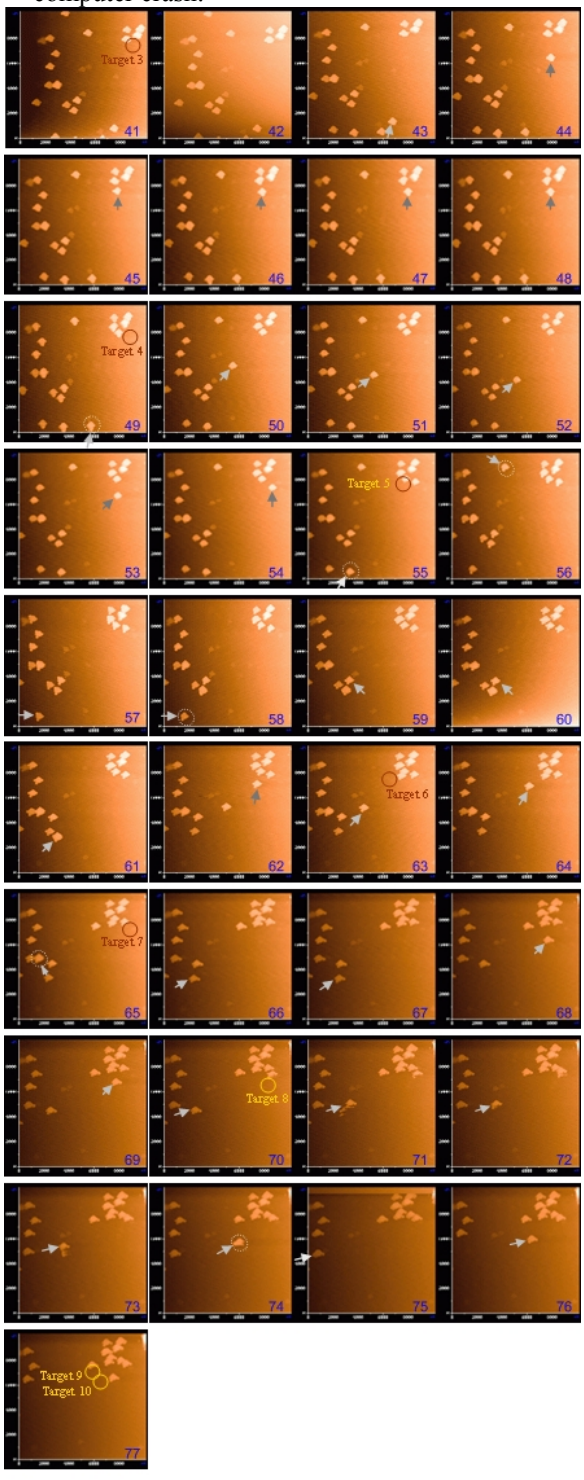

Part 3. Pushing particles to target 11 are shown from

Pictures 78 to 107. Using twenty-three times push a particle to target 11. The reason of using such more times is that tip lands too deeper to lose positioning accuracy. Under each positioning, sample surface was scraped by tip. Moreover, during positioning, tip location was changed due to surface friction.

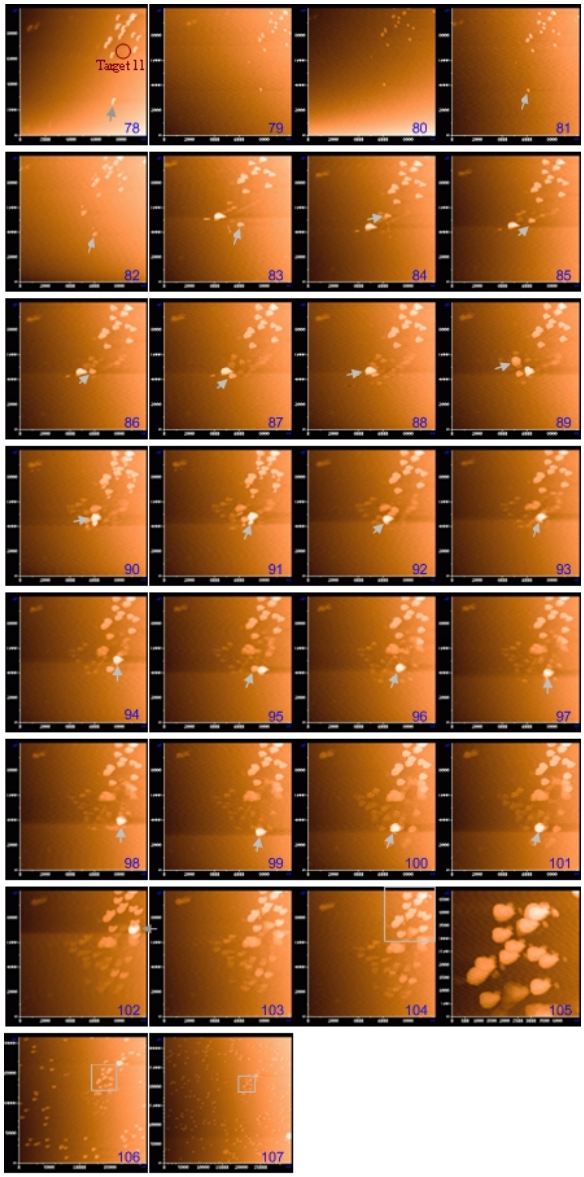

Fig. 22 Process of pushing nanoparticles.

According to Parts 1 and 2, nanoparticles are adsorbed by the tip almost at pushing up the inclined substrate, where are shown at Pictures 38, 49, 56, 58, and 74. There are only two cases that nanoparticles are adsorbed by the tip in pushing down the inclined substrate, as depicted in Pictures 14 and 65.

6. CONCLUSION

This study uses SMC with LQE observer to deal with input disturbance and measurement noise and fuzzy control to compensate displacement error during nanoparticle manipulation. Simulation and Experimental results have demonstrated performances of stage-position control and nanoparticle manipulation.

ACKNOWLEDGEMENT

This work was supported by National Science Council of Republic of China under grant no. NSC93-2212-E-009-023.

REFERENCES

1. Sitti, M. and Hashimoto, H., “Controlled Pushing of Nanoparticles: Modeling and Experiments”, *IEEE/ASME Trans. on Mechatronics*, Vol. 5, No. 2, June 2000.
2. Sitti, M., “Atomic Force Microscope Probe Based Contorlled Pushing for Nanotribological Characterization”, *IEEE/ASME Trans. on Mechatronics*, Vol. 9, No. 2, June 2004.
3. Gao, W. B., Wang, Y. and Homaifa, A., “Discrete-Time Variable Structure Control Systems”, *IEEE Transactions on Industrial Electronics*, Vol.42, No.2, April, 1995.
4. Junno, T., Deppert, K., Montelius, L., and Samuelson, L., “Controlled Manipulation of Nanoparticles with an Atomic Force Microscope”, *Appl. Phys. Lett.*, Vol. 66, No. 26, pp. 3627-3629, June 1995.

可供推廣之研發成果資料表

□ 可申請專利　■ 可技術移轉　日期：2005 年 7 月 30 日

國科會補助計畫	計畫名稱：操作奈米粒子之動力學分析與控制（III） 計畫主持人：　呂　宗　熙 計畫編號：　NSC93－2212－E－009－023 學門領域：機械固力
技術/創作名稱	呂　宗　熙
發明人/創作人	
技術說明	中文：為了機電元件的微小化與生化方面的應用，奈米科技技術運用的重要性也隨著與日俱增。但也由於目前的奈米技術還尚未發展成熟，因此利用奈米操控術來組成奈米級之機電元件與生化 DNA 重組是很重要的研究主題。本研究採用針對模型之不確定性及外界干擾有強健性的順滑模態控制去控制平台，利用閉迴路 X-Y 精密平台的應變計回饋訊號使探針能準確的推動於傾斜面上的奈米粒子。為了補償可能發生的探針與奈米粒子失去接觸，本研究擷取原子力顯微鏡中探針懸臂樑撓曲時，雷射光呈現於四象儀光偵測器的回授電壓訊號，然後使用模糊控制器對此訊號作 X-Y 平台的定位控制，建立一個穩定和高精度的粒子推動系統。
	英文： To develop nanotechnology, nanoparticle manipulation plays an important role in the assembly of nanoelements. This study aims to manipulate nanoparticles using an atomic force microscope and an XY positioning stage. Strain gauges serve as sensors to measure the travel distance of piezo-drivers in an X-Y stage in an atomic force microscopy system. Nanoparticles are pushed based on sliding mode control whose robust properties can deal with model uncertainty and disturbance. In addition, a fuzzy controller is responsible for compensating “tip-particle contact loss”, so as to establish an accurate and stable manipulation system. Experimental results demonstrate pushing nanoparticles on inclined substrates, different limited scanning ranges with different slope angles, and removing and remaining nanoparticles on inclined substrates.
可利用之產業及可開發之產品	原子力顯微鏡和電子穿隧顯微鏡、微探針。
技術特點	本研究擷取原子力顯微鏡中探針懸臂樑撓曲時，雷射光呈現於四象儀光偵測器的回授電壓訊號，然後使用模糊控制器對此訊號作 X-Y 平台的定位控制，建立穩定和高精度的粒子推動系統。

推廣及運用的價值	本研究發揮微探針和精密移動平台的運動特性，能夠應用於從事奈米級之機電元件與生物科技組裝和製造。